DOI: https://doi.org/10.37434/tpwj2025.04.05

ELECTRON BEAM WELDING OF GAS VALVE ELEMENTS FROM Mo–Ti–Zr ALLOY

V.I. Zagornikov, V.M. Nesterenkov, K.S. Khripko, O.N. Ignatusha

E.O. Paton Electric Welding Institute of the NASU
11 Kazymyr Malevych Str., 03150, Kyiv, Ukraine

ABSTRACT

The technological techniques of electron beam welding (EBW) are considered, the application of which would allow obtaining the required quality of joints of gas valve parts made of Mo–Ti–Zr (TZM) alloy, which is used in difficult conditions of the nuclear industry. It is known that in order to produce a welded joint with relatively high ductility indices, the oxygen content should not exceed thousandths of a percent. Alloys produced by vacuum arc and electron beam melting are used for welded structures. They have a much lower tendency to form porosity in welded joints than similar alloys made by powder metallurgy methods. Such alloys can be welded, but these joints cannot always be used under dynamic loads. When choosing the optimal welding technique for gas valve parts, technical requirements for edge preparation, quality of welded joints, availability of appropriate equipment and technological tooling were taken into account. The problems of assembly and subsequent welding of gas valve parts made of Mo–Ti–Zr (TZM) alloy revealed during the investigations caused the need in changing design of the joints. As a result, a scheme for welding gas valve parts was proposed, which uses flanging of weld butt edges. This led to optimizing the penetration shape. The proposed welding parameters and flange geometry made it possible to lower the degree of saturation of the weld metal with gases due to the reduction in the penetration depth under the conditions of rapid heat removal and, as a result, to produce sufficiently high-quality welded joints. In addition, with all the variety of technological techniques used during the investigations, the priority of the correctly selected design of the circumferential butt and the accuracy of the welding assembly was proven.

KEYWORDS: Mo–Ti–Zr (TZM) alloy, electron beam welding (EBW), microstructure, porosity, gas valve, flanging of welded edges

INTRODUCTION

Molybdenum and its alloys have many unique characteristics, which makes them indispensable in such areas as aerospace, power, chemical defense, and metallurgy. The use of molybdenum-based alloys in nuclear engineering in future thermonuclear reactors is challenging, since these alloys, along with high strength and fatigue resistance at high temperatures, have good thermophysical properties and are not activated by irradiation. The use of molybdenum as the base of a structural alloy is constrained by its two disadvantages: easy oxidation at temperatures above 500–700 °C and reduced ductility at room temperature [1]. Molybdenum alloying practically does not help to eliminate the first drawback, but it can significantly increase the recrystallization temperature, strength, and creep resistance at high temperatures, and, in case of dispersive hardening, for example, with lanthanum oxide, increase heat resistance and improve the ductile properties (reduce the brittleness threshold).

It is known that the presence of impurities in the base metal in quantities significantly exceeding their solubility limit is an objective obstacle in producing high-quality welded joints on molybdenum alloys [2, 3]. The quality of welded joints, mechanical characteristics of welds, and especially their low-temperature ductility are very sensitive to the structural state of the initial material. To obtain a sufficiently high ductility of the welded joint, especially at low temperatures, it is necessary that the base metal has a homogeneous initial structure and sufficiently high resistance to ductile-to-brittle transition. This can be achieved by selecting the most favorable conditions for preliminary hot treatment of the metal to be welded (for example, rolling mode for sheet alloys), as well as heat treatment before welding (for example, for molybdenum alloys at a temperature of 1400–1800 K, depending on their composition) [4].

It should also be taken into account that any alloys of refractory metals of the VIa subgroup of the periodic table (including molybdenum alloys) produced by vacuum arc or electron beam remelting have a much lower tendency to form porosity in welded joints than similar alloys produced by powder metallurgy. This is usually predetermined by the fact that powdered metals have a higher content of gas impurities. However, welded joints made with powdered alloys, even with lower impurity content than those made with conventionally produced alloys, tend to reveal porosity. During the welding process, gases can expand rapidly in the molten pool, which seriously degrades the quality of welded joints of molybdenum and molybdenum alloys [5–7].

The use of powdered Mo–Ti–Zr (TZM) molybdenum alloy is constrained by its low processability and especially weldability. The weld and heat-affected zone (HAZ) are relatively wide, and the grains are highly coarsened after welding, so penetration impurities such as C, N and O are fully diffused and concentrated at the grain boundaries, resulting in a significant weakening of the bond strength at the grain boundaries. At the combined effect of intrinsic brittleness of materials and segregation of impurities at grain boundaries, the sensitivity to welding cracks is high, and the strength and ductility of joints of molybdenum and its alloys are low [8, 9]. At even the lowest level of impurities-gases in the weld, it is impossible to ensure sufficient ductility of welded joints with their typical coarse-crystal structure and eliminate the tendency to cold crack formation. Producing high-quality welded joints requires the use of alloys doped with expensive elements that reduce the harmful effect of impurities on welds (e.g., deoxidizers such as titanium, zirconium, etc.) and improve their structure (e.g., with rhenium) [10]. Therefore, parts or structures made of molybdenum and molybdenum alloys often have to be manufactured by powder metallurgy rather than by welding from parts.

Since the most perfect shielding of the weld from atmospheric gases is achieved in EBW, this method is most effective for joining chemically active refractory metals, since it is performed in a vacuum and provides relatively low heat input. For refractory and chemically active metals, the possibility of their preliminary cleaning by degassing in a vacuum is of great importance. To reduce contamination of the weld metal, welding is usually performed without filler metal.

The relatively small width of the HAZ becomes a great advantage in welding refractory metals such as molybdenum. The weld and the near-weld zone (recrystallization zone) are much less strong and have a much higher ductile-brittle transition temperature than the base material itself. This difference in strength leads to a concentration of strain in the weld zone, and the triaxial stress created by the confinement of the base metal can initiate fracture. It should be noted that although vacuum electron beam welding facilitates the removal of impurities and gases, it increases the evaporation of alloying elements.

Experimental works are mainly devoted to clarifying the role of welding conditions and parameters, or more precisely, their role in improving weld quality (tempering brittleness, limitation of continuous grain growth). The information provided in the literature on the effect of heating and cooling rates on the low-temperature ductility of molybdenum alloys is contradictory. Morito et al. [11] compared the ductility of HAZ in welding molybdenum alloys (Mo > 99.9 wt.%) under two heat treatment conditions, i.e., at cooling in a furnace and rapid cooling by quenching. It was found that rapid cooling after welding can significantly reduce the ductility of the HAZ of a welded joint of molybdenum alloys, mainly because grain boundary segregation in the HAZ is greater at rapid cooling by quenching. Stutz et al. [12] systematically studied the influence of EBW process parameters on the sizes of the melting zone and HAZ, pore and crack sensitivity in a butt welded joint made of TZM alloy with a thickness of 2 mm.

The results show that pore formation is seriously affected by excessive heat input during welding. A small (insignificant in terms of the degree of manifestation) heat input can not only suppress pores, but also obviously reduce the grain size in the melting zone.

It was found in [5] that although it is not possible to completely avoid pore formation in welding powdered metals, the porosity in the melting zone at a limited heat input is significantly reduced. By increasing the welding speed and reducing the heat input, the ductility of the welded joint of molybdenum can be significantly improved by refining the weld structure. This results in a significant reduction in the thickness of the MoO_2 oxide film located at the grain boundaries. Reducing the thickness of the oxide film along the grain boundaries increases the intercrystalline bonds and, consequently, the ductility [13].

THE AIM

of the research is to develop a technique for electron beam welding of circumferential welds while joining gas valve parts made of Mo–Ti–Zr molybdenum alloy.

RESEARCH METHODOLOGY

EBW opens up the possibility to clean the metal from gases before welding by heating the butt edges with a defocused electron beam. Hydrogen is removed most successfully, oxygen and nitrogen are removed least successfully, and only from the surface layers of the metal. It is assumed in [14] that preheating of the butt reduces pores and helps to remove surface contaminants of adsorbed gases that cause porosity, calmer formation of the substructure in the weld, and prevents the formation of cold cracks in the studied alloy due to the overall expansion of the future welding zone. It is noted that heating at temperatures above 900 °C is inappropriate due to possible deformation of parts and the beginning of the recrystallization process.

A necessary condition for producing high-quality welded joints is the accuracy of the assembly (and fixation) of the butt for welding. For example, when welding circumferential joints made of molybdenum

alloys, it is recommended that the edge displacement should not exceed ±50 μm. Assembly of parts for welding should be carried out in particularly precise devices. These devices must ensure that the edges to be welded are pressed tightly together, as effective heat removal is required to reduce welding deformations [15]. The Mo–Ti–Zr alloy, which is produced by powder or pellet metallurgy, guarantees chemical compliance of the basic alloying elements and mechanical strength in the delivery state, i.e. it can be used for technical tasks that do not require metal remelting. However, this material is problematic for structures joined by electron beam welding.

In our work, the technological methods of electron beam welding are considered, the application of which makes it possible to obtain the required quality of welded joints of gas valve parts made of Mo–Ti–Zr alloy, including the conditions for assembling parts for welding. We studied the effect of the joint type of parts with circumferential welds produced by electron beam welding on the strength and ductility of such a joint. Such joints are the most critical in terms of crack formation and are problematic at an attempt to produce a serviceable welded joint. The work also touched the issue of the influence of gases, primarily oxygen (O_2) on weldability at different types of gas valve part joints produced by electron beam welding.

The design of the nipple joint to the gas valve body is fixed in the assembly fixture on a welding rotary positioner (rotator). The rotator being a part of the installation kit allows mounting in two spatial positions: with a horizontal or vertical axis of rotation (Figure 1). Using an indicator post and a clock-type indicator, the nipple was aligned with the positioner's axis of rotation. The deviation was within 0.1 mm.

Welding was carried out in an electron beam installation of the KL-211 type with a pressure in the working volume of the chamber not higher than $5 \cdot 10^{-4}$ mm·Hg. The accelerating voltage is set at a level of 60 kV. Electronic optics was used, designed for 500 mA of electron beam current. It included a metal cathode with an emitting surface with a diameter of 3 mm. The experiments were carried out at a working distance of 250 mm from the end of the welding gun to the facial surface of a product.

The influence of the input energy was studied, namely three fixed values of the welding speed: 5, 10 and 15 mm/s, in the range of heat input q = 320–540 J/mm.

Figure 1. KL-211 installation. Device for assembling and welding gas valve simulator in two spatial positions: with horizontal (*a*) and vertical axis of rotation (*b*)

Metallographic examinations of the weld penetrations were carried out in the Neophot-32 optical microscope at different magnifications. The grain size was calculated by the linear method. The hardness of the phase components was measured in the M-400 microhardness tester from LECO, the load was 1 N, the holding time was 10 s.

The composition of the alloy was checked using an X-Ray Spectrometer X'Unique II — Rh 80 kV LiF220 Ge111 TIAP. The obtained data of chemical and gas analysis of the alloy are presented in Table 1.

The first EBW test specimens showed elevated brittleness of the weld metal and the base metal itself. In order to prevent the formation of unacceptable pores and cold cracks in the studied alloy, the techniques were used, which are discussed below.

The initial selection of welding modes was carried out on a set of 50×240×25 mm plates with non-through and through penetration. To obtain an acceptable formation of a facial weld bead, the specimens were welded by changing the parameters of the elec-

Table 1. Chemical composition of molybdenum TZM alloy

Elements	Mo	Ti	Zr	Al	Si	Cr	La	C	O_2	N_2
wt.%	≤99.23	≤0.53	≤0.13	≤0.046	≤0.041	≤0.013	≤0.037	≤0.031	≤0.0092	≤0.001

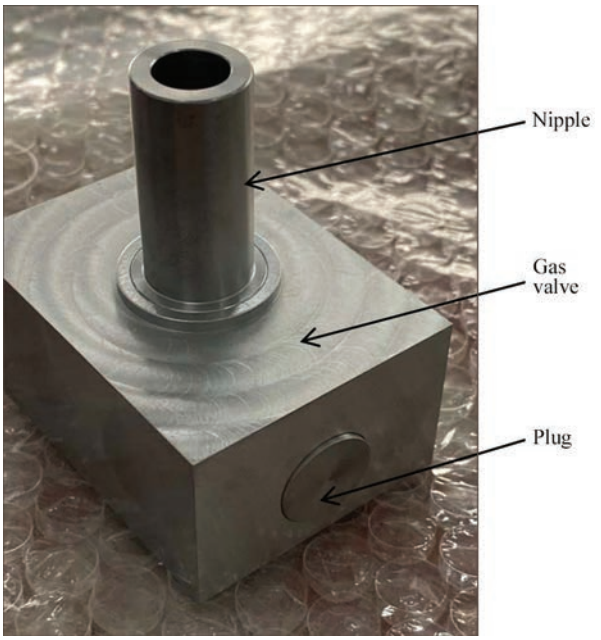

Figure 2. Assembled parts of Mo–Ti–Zr alloy gas valve simulator

tron beam focusing, its current and welding speed. In accordance with the recommendations [14], to increase the deformability of the metal, preheating of the joint was used. The reference surface temperature was 900 °C. The following mode of electron beam heating of the welding zone was selected: accelerating voltage 60 kV, beam current 30 mA and heating time 12 min.

Each joint was welded separately, followed by cooling in vacuum for 30 min. After welding, mechanical tensile tests were performed on the specimens at temperatures of 20 and 1200 °C.

The influence of the welding input energy per unit time was studied. Different welds were produced by varying the beam current from 30 to 60 mA and the welding speed from 5 to 15 mm/s. The use of the focused electron beam is not rational, since it does not allow obtaining the required shape of the penetration zone. An acceptable level of electron beam concentration reduction of ±7 mA of the focusing current from its value at a sharp focusing (measured at minimum beam power) was experimentally determined. The weld geometry was optimized by using technological electron beam scanning.

Modes of welding the nipple with the gas valve body and two cylindrical plugs on opposite walls of the same body were tested (Figure 2).

ANALYSIS OF RESULTS AND TECHNOLOGICAL RECOMMENDATIONS

MICROSTRUCTURE OF WELDED JOINTS OF Mo–Ti–Zr *ALLOY*

Due to the effect of the thermal cycle of welding, grain growth in the near-weld zone, thickening of intergranular interlayers and their enrichment with impurities and a sharp increase in the brittleness of the metal in this zone occurs. The alloy is sensitive to the thermal cycles of welding and, above all, to the cooling rate, which is associated with the precipitation of the second phase. Therefore, the orientation of the weld metal crystals, the shape of the grain boundaries and the level of residual stresses mainly depend on the welding speed.

It was found that low heat input (q = 320 J/mm) due to increased welding speed leads to significant grain refinement in the melting zone.

Reduction in the speed to lower than 5 mm/s (q = 540 J/mm) increased the formation of pores. In addition, more pores are fixed in the fusion zone than in the volume of the weld. Also, welds with a high "wedge-like" penetration and a large total width of the penetration zone are formed. With an increase in the welding speed, both the average size of pores and their number decrease. On the other hand, the welding speed was limited, because welding at a speed exceeding 15 mm/s led to a decrease in the stability of the welded joint formation and the appearance of defects in the form of oscillations of the facial bead surface (Figure 3, *c*). At the same time, without scanning of the electron beam or at a small scanning width, a very sharp weld root with a high probability of root defects is naturally formed. By increasing the scanning width to 0.8 mm, a compromise was achieved between the

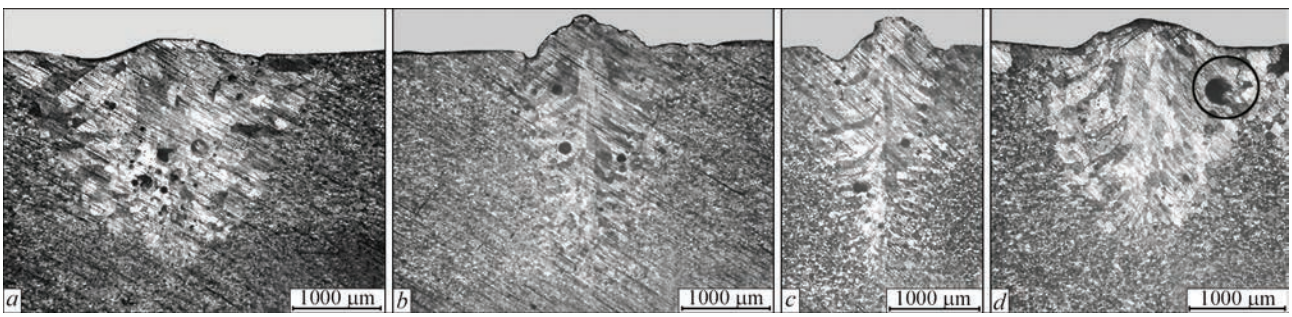

Figure 3. Penetration zone (×30): *a* — V_w = 5 mm/s, A_s = 0.8 mm, I_w = 45 mA, q = 540 J/mm; *b* — V_w = 10 mm/s, A_s = 0.8 mm, I_w = = 55 mA, q = 330 J/mm; *c* — V_w = 15 mm/s, A_s = 1.6 mm, I_w = 80 mA, q = 320 J/mm; *d* — with repeated penetration at V_w = 5 mm/s, A_s — 0.8 mm, I_w = 40 and 45 mA, respectively

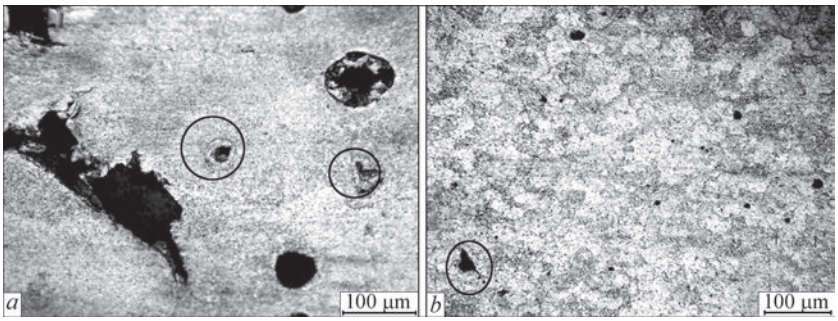

Figure 4. Defects in weld metal (*a*), defects in HAZ metal (*b*) (×200)

total width, the "wedge-like" shape of the penetration zone and the shape of the weld root (Figure 3, *a, b*).

In all the investigated weld penetrations, in addition to the macropores mentioned above, micropores were found in the weld metal. Defects are mainly globular in shape, but there are also single defects of irregular shape (Figure 4, *a, b*). The size of defects varies within 38–375 μm.

In the HAZ and in the base metal of the studied specimens, single micropores were also found, as well as inclusions of various sizes and in large amount. The bulk of these inclusions has a size of 2.5–5.0 μm, quite a lot of inclusions of 18–20 μm and a small number of large inclusions of 37.5–50 μm. The hardness (*HV*1) of the inclusions is in the range of 10180–12500 MPa.

To confirm the influence of an increased content of gas impurities in the base metal on the weld porosity, experiments on double metal remelting were conducted. We performed experiments on double metal remelting: both welding passes at similar parameters, but the first pass at 0.8–0.9 of the beam power at the second pass. I.e., at the second pass we completely remelted the weld metal from the first pass and touched a small interlayer of previously unremelted base metal. As was expected, in the center of the weld metal after remelting the number of pores decreased noticeably, but near the fusion zone there are still many of them as before (Figure 3, *d*).

Apparently, despite some «refining» of the weld metal as a result of the first pass, the high concentration of gases in the boundary interlayer and partial diffusion of gases from the base metal, as before, initiate the propagation of pores, and increased gaps — cracks.

The structure of the weld in all the studied cases represents coarse grains, elongated from the center of the weld in the direction of heat removal (Figure 3). The size of grains in the weld at a welding speed of 5 mm/s is 185–250 μm, and at a speed of 10 mm/s — 100–180 μm. The weld microstructure is everywhere two-phase, consisting of a light α-phase matrix (solid solution based on molybdenum) and an excess phase in the form of small inclusions of irregular shape (Figure 5, *a*).

The hardness (*HV*1) of the weld metal at a welding speed of 5 mm/s is 2280–2360 MPa, and near the fusion line it decreases to 2060 MPa. The hardness of the weld metal at a welding speed of 10 mm/s is somewhat higher — 2360–2660 MPa, and near the fusion line — 2280 MPa, respectively. The fusion line is not pronounced.

The HAZ microstructure is two-phase with embeddiments of inclusions described above (Figure 4, *b*). The grain size at a welding speed of 5 mm/s is 90–125 μm, the hardness (*HV*1) is 2210–2270 MPa, and at 10 mm/s — 60–100 μm and 2180–2430 MPa, respectively. The structure of the base metal is fibrous, retains the deformation texture, consists of two phases and precipitations (inclusions), the grains are not pronounced (Figure 4, *c*), the hardness (*HV*1) of the metal is in the range of 2790–3220 MPa (Figure 6).

All welded joints of a gas valve require a relatively small depth of partial penetration, namely 3–4 mm. With an increase in the thickness of the welded metals, serious difficulties arise due to overheating of the weld metal, an increase in HAZ and, as a result, the

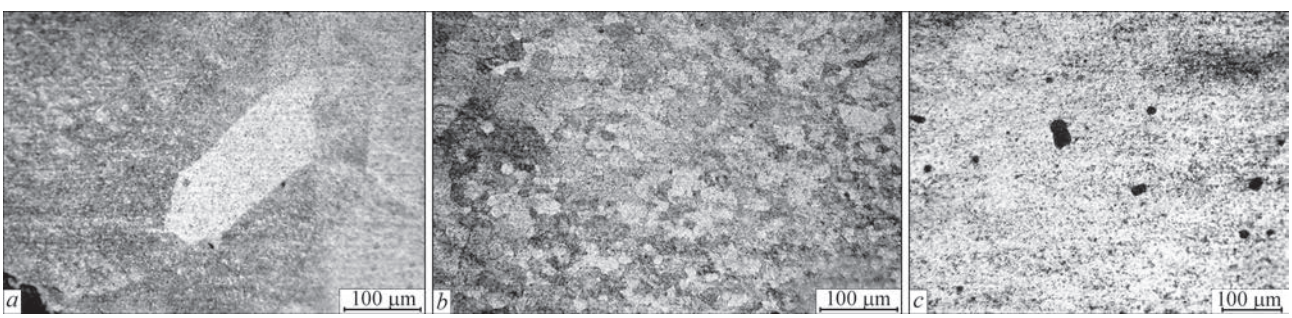

Figure 5. Typical structure of weld metal (*a*), HAZ metal (*b*), base metal (*c*) (×200)

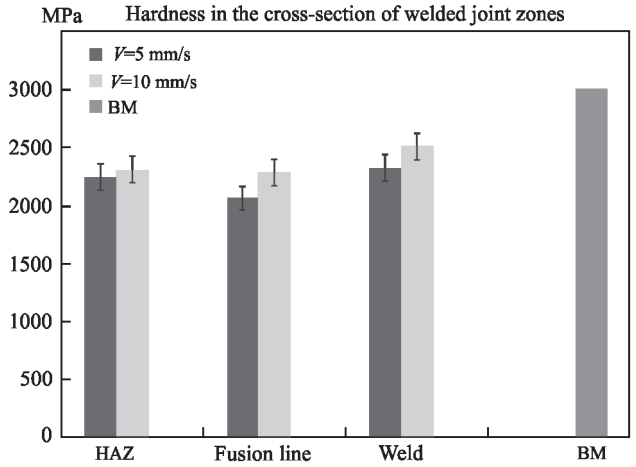

Figure 6. Average hardness of different welded joint zones at EBW and in the base metal

formation of pores and cracks. The use of the electron beam scanning technology made it possible to obtain the required shape of the penetration zone with a much lower tendency to porosity formation.

Taking into account the results of the choice of modes on plane specimens, a number of welding experiments were carried out to select and work out the welding modes of gas valve parts, namely three joints: a nipple with a valve body and two plugs on the opposite walls of this body. Two 16-mm diameter plug holes and one nipple connection were welded to a casing hole of 20 mm diameter. To exclude possible crystallization cracks, the shortest possible sections of the electron beam current input and output were selected. The actual valve parts were assembled in a device that allows welding of all parts of the assembly simultaneously.

GENERAL SEQUENCE OF WELDING-ON FITTINGS TO THE VALVE BODY

Welding algorithm: increment in the welding current to the specified value, holding this current constant during a 360° angular welding movement, then overlapping the initial section and, finally, gradual reduction in the welding current. The overlap length was chosen to prevent lack of penetration in the initial section of the joint and to prevent the formation of an end crater.

Parameters of local tacks (sections 10 mm each): beam current — 25 mA; beam focusing current — 560 mA; movement speed — 5 mm/s; circular beam scanning diameter — 1.0 mm.

The operation for preparing preheating of the butt remained relevant. To provide a uniform heating of the body and nipple, the electron beam was shifted from the butt towards the body by 8 mm. Heating parameters: beam current — 25–30 mA; beam focusing current — 500–510 mA. Movement speed — 5 mm/s; circular beam scanning diameter — 8 mm; number of passes — 15; reference temperature on the surface — 900 °C.

After heating, the subprograms for continuous tack welding and full penetration were run sequentially. Parameters of continuous tack: welding current — 25 mA, focusing current — 510 mA. Welding speed: 5 mm/s. Beam scanning — diameter circle of 1.0 mm.

Welding mode parameters were changed within the following limits: welding current — 30–48 mA, welding was performed with a defocused electron beam, focusing current — 560 mA. The welding (rotation) speed was 7–10 mm/s. Beam scanning — a circle with a diameter of 0.5–1.0 mm (Table 2).

Table 2. Parameters of preheating and EBW modes for gas valve parts

Parameters of preheating on the surface	
Nipple (bushing)	Plugs
Temperature — 900 °C; Number of passes — 15; Rotation speed — 5 mm/s; Current — 25–30 mA; Beam scanning — 8.0 mm circle, the beam is shifted at 8 mm towards the body from the joint; Focusing current — 500–510 mA	Temperature — 900 °C; Number of passes — 15 first, 10 second; Heating time — 10 min; Rotation speed — 7 mm/s; Current — 5–8 mA; Beam scanning — 2.0 mm circle; Focusing current — 500 mA

EBW stages	EBW stage parameters							
	Nipple (bushing)				Plugs			
	V_w, m/s	I_w, mA	I_f, mA	Beam scanning, appearance, size, mm	V_w, m/s	I_w, mA	I_f, mA	Beam scanning, appearance, size, mm
Short tacks (10 mm)	5	25	560	Circle, 1.0	5	25	510	Circle, 1.0
Solid tacks	5	25	570	Circle, 0.5	5	25	560	Circle, 0.5
Main weld	7–10	45–48	560	Circle, 0.5	10	40	560	Circle, 0.5
Smoothing pass	12	30	700	10	12	30	700	10

During the assembly, it was found that the gap value between the gas valve parts to be welded reached 0.1 mm, which does not meet the requirements specified for assembling units for EBW made of molybdenum alloys. The initial condition of providing the accuracy of the butt assembly was not met. Due to an increased gap in the butt during assembly, the risk of arising shrinkage cracks and root defects in the area with a crater increased. Nevertheless, the valve fittings were welded. Repeated penetration allowed forming the upper bead, but to correct the root defects, it was necessary to drill out the plug and insert a new part with a subsequent rewelding. Such a long and labour-intensive process was recognised as poorly manufacturable and was not considered further.

The research results showed that low heat input helps to delay pore growth and reduce grain size in the melting zone. The heat input was decreased by reducing the welding current, increasing the speed to a certain limit and optimizing the shape and sizes of the electron beam scanning.

Preparation of end surface of edges to be welded to reduce the porosity is necessary but not sufficient. In addition, preheating and remelting of this joint turned to be ineffective as a method of combating metallurgical pores. These operations do not solve the problem of increasing the ductility of a welded joint, but they were not cancelled due to the possible prospect of having a positive impact on the rate of phase and structural transformations without deteriorating the weld structure. It was necessary to search other ways to improve the weld quality. Difficulties that appeared during forming welds on gas valve parts made it necessary to change the design of the welded joint body-nipple and body-plugs.

It is known that one of the widely used technological methods aimed at increasing the resistance of the weld metal to pore formation and crystallization cracks is the change in the penetration shape (ratio of weld width to penetration depth). The carried out studies have shown challenge in terms of joining with flanging of welded edges, where primary crystallites are joined by side faces rather than apexes in the process of melt solidification. Such welds are more resistant to cracking.

STAGES OF WELDED ASSEMBLY MODERNIZATION

In the process of step-by-step changing in the assembly scheme and the design of the welded assembly, a solution was found to improve the manufacturability of the welding process. Figure 7, *a–c* shows the se-

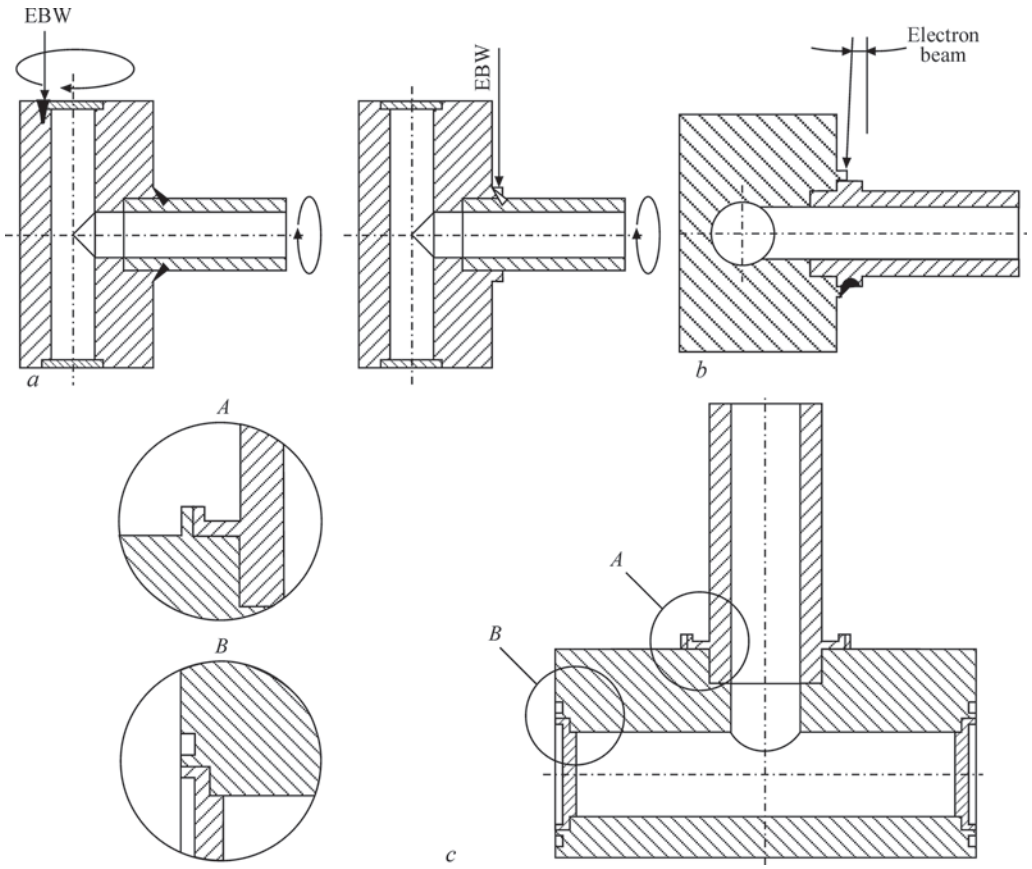

Figure 7. Three stages of modernization of the assembly welded joint design: fish-mouth welding of the nipple with the body is replaced by a scheme with a "collar" fused to the nipple wall, the body with plugs is fish-mouth welded (*a*), the nipple is modified for welding with an inclined electron beam (*b*), modernization of fitting joints in the form of flanging the joint edges (*c*)

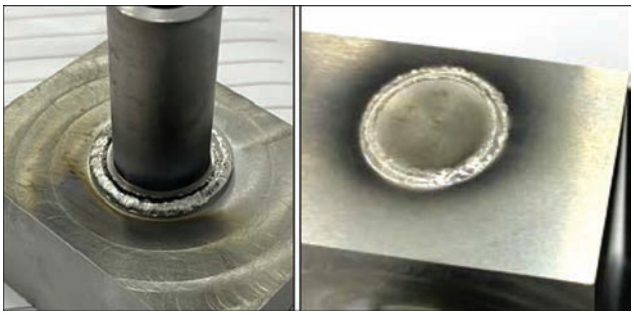

Figure 8. Formation of circumferential welds with edge flanging, imitating nipple-body and plug-body joints

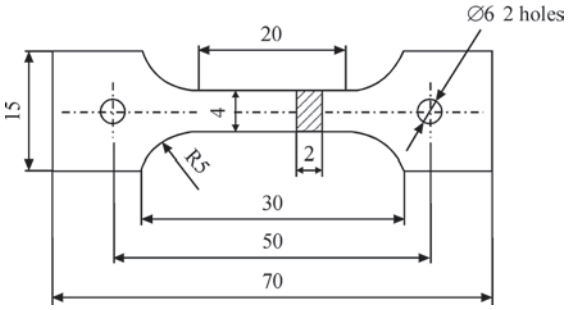

Figure 10. Tensile test specimen

quence of step-by-step transformation of joint variants, which was carried out as a result of the carried out studies.

Variant "*b*". The deflection angle and focus location of the electron beam have been clarified. It became possible to weld three butts within one evacuation of the welding chamber. However, the subsequent welding of gas valve parts, fittings and plugs, due to inacceptable gaps in the butt, did not provide the required tightness, as was shown by hydraulic tests. Therefore, it was proposed to fit the H7/p6 joint, which provides a small guaranteed tension in the joint. The operations to eliminate the gap in the butt joints before welding by high-precision grinding of gas valve parts provided the highest guaranteed tightness of the joint by obtaining the required fit.

Variant "*c*" was accepted as the basic one, and the drawings of gas valve parts were made in accordance with Figure 7, *c*. This variant simplifies the positioning of a part before welding. There is no need to weld with an inclined beam, as was assumed in one of the previous schemes.

All welds made with a "tight" joint (without a gap in a butt) had a fairly stable formation of the outer bead (Figure 8).

The advantages of this joint design include, first of all, the fact that it allows radically reducing the heat input during welding. The use of edge flanging makes it possible to achieve the most favourable ratio of the pool depth to its width. I.e., welding can be performed with a fairly wide and shallow weld at a moderate electron beam concentration. The presence of root defects in this case is not significant. Due to the thermophysical properties of the molybdenum alloy, the penetration shape of such welds in the cross-section remained rather wedge-shaped, but with a rounded root part. Figure 9 shows penetration shapes on the selected welding modes.

Selected modes for producing circumferential welds of joining fittings to the valve body:

- for plugs — V_w = 10 mm/s, focusing current 560 mA, beam scanning A_s = 0.5–0.8 mm, I_w = = 45–55 mA;
- for nipple — V_w = 7 mm/s, focusing current 570 mA, beam scanning A_s = 0.8–1.0 mm, I_w = = 30–45 mA.

Molybdenum is very sensitive to undercuts and therefore, they should be avoided as well as craters. The use of an additional smoothing pass reduces possible stress concentrators (including undercuts) and porosity in the most dangerous near-surface area. A smooth transition from the weld to the base metal is provided. The weld width is uniform, the surface is smooth and mirror-like on the facial side, and craters are absent.

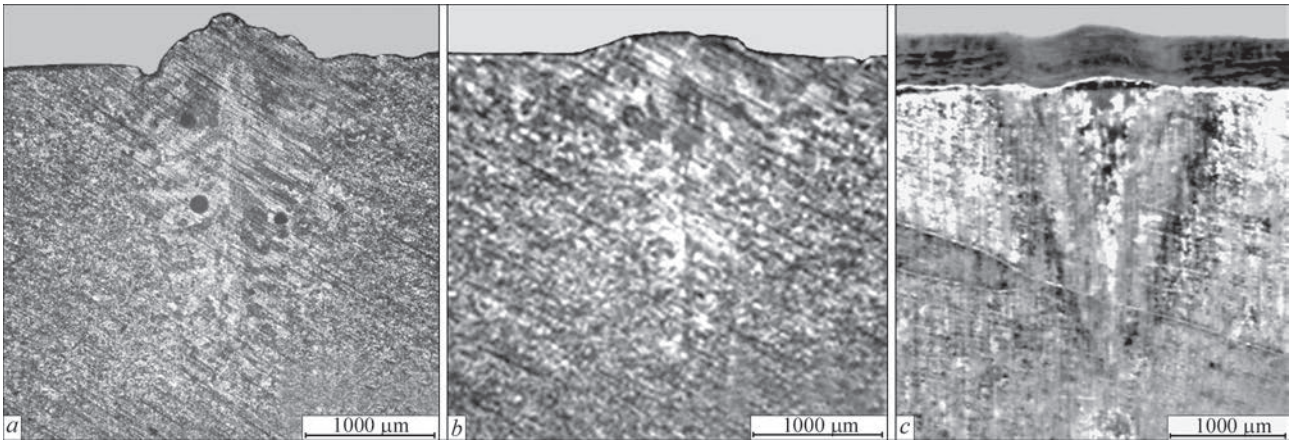

Figure 9. Cross-sectional view of the penetration zone under selected modes of producing circumferential welds: *a* — for plugs: V_w = = 10 mm/s, A_s = 0.8 mm, I_w = 55 mA; *b* — for nipple: V_w = 7 mm/s, A_s = 0.8 mm, I_w = 30 mA; *c* — the same with a smoothing pass V_w = 10 mm/s, I_w = 45 mA

Table 3. Mechanical properties of base metal and welded joint metal at different test temperatures

Test temperature, °C	$\sigma_{t.BM}$, MPa	$\sigma_{t.WJ}$, MPa	K_{str}
20	570	490	0.85
1200	189	144	0.76

Notes. 1. Average values of testing four specimens are given. 2. Ultimate tensile strength was tested on plane specimens, Figure 10. 3. Strength factor — $K_{str} = \sigma_{t.WJ}/\sigma_{t.BM}$.

The prospect of using welding modes with adjustable distribution of the electron beam power density along the butt edges by rapid oscillation from one extreme position to another is noted [15, 16].

Accordingly, the mode of smoothing passes along the facial side of the preliminary cooled weld: V_w = = 12 mm/s, focusing current — 700 mA, transverse beam scanning with adjustable distribution of its power density along the scanning trajectory A_s = 10 mm, I_w = 30 mA.

The disadvantages of the above design may include the difficulty of manufacturing welded assemblies and the inability to weld the entire assembly within a one evacuation.

The technological process of joining gas valve parts was completed by heat treatment in a furnace for a complete removal of residual welding stresses. Treatment mode: heating rate 25 °C/min = 0.42 °C/s to a temperature of 1150 °C, holding within 60 min, cooling in the furnace.

After welding and heat treatment, X-ray inspection of welded joints was carried out. The X-ray inspection showed a maximum pore diameter of 0.723 mm. The minimum distance between pores is 4.345 mm. Each valve has three welds. After the works on modernization of the design of welded assemblies and optimization of the welding mode, the number and size of pores became non-critical for the gas valve serviceability. X-ray inspection of the welds showed the maximum pore diameter in the range of 0.35–0.43 mm. Their number and sizes do not exceed the requirements of the technical specifications.

The hydraulic tests were also carried out on the welded gas valves. All valves passed the tests successfully. The pressure of 20 MPa was maintained for 2 min without leakage, which meets the requirements of the technical assignment.

After testing the welding technology for the new design of the assembly joint, as well as mechanical tests on industrial specimens, this design and the parameters of EBW welding of gas valve joints of real valve parts were finally selected.

CONCLUSIONS

1. Porosity is a complex problem in fusion welding of molybdenum and its alloys because of the already existing inner defects, first of all related to the powder metallurgy process. Preheating of the butt with a defocused electron beam leads to an overall volume expansion of the future welding zone and facilitates the removal of surface contaminants from adsorbed gases. The latter can significantly reduce the formation of pores, but does not guarantee their complete elimination.

2. The carried out experiments confirmed that the formation of metallurgical pores in EBW, in addition to the influence of harmful gas impurities, is closely related to the assembly conditions, welding speed and weld cross-sectional shape. Preparing end surface of the welded edges and the accuracy of the butt assembly are essential conditions for producing a high-quality welded joint, especially with a satisfactory combination of strength and ductility.

3. The results of the analysis of the mechanical properties and structural state of the welded joints confirmed the correct choice of welding mode parameters with minimum values of the input energy and adjustable distribution of power density of the electron beam scanning trajectory. The use of this mode made it possible to reduce the grain size and a number of voids in the melting zone. This shortens the length of the heat-affected zone, reduces the size of crystallites, and changes the crystallization pattern of the weld metal, which has a favourable effect on the mechanical properties of welded joints, and especially on the low-temperature ductility.

4. To obtain the required quality of welds, changes were made to the design of the gas valve welded joints. A series of welding experiments on the joints of gas valve parts made it possible to modernize the design of welded assemblies using flanging of welded edges, which allowed producing serviceable circumferential welded joints.

REFERENCES

1. Trefilov, V.I., Milman, Yu.V., Firstov, S.A. (1975) *Physical basis of the strength of refractory metals.* Kyiv, Naukova Dumka [in Russian].
2. Platte, W.N. (1956) Influence of oxygen on soundness and ductility of molybdenum weld. *Weld. J.,* 35(**8**), 369–381.
3. Platte, W.N. (1957) Effects of nitrogen on the soundness and ductility of welds in molybdenum *Weld. J.,* 36(**6),** 301–306.
4. Gurevich, S.M. (1975) *Welding of chemically active and refractory metals and alloys.* Kyiv, Naukova Dumka [in Russian].
5. Miao-Xia Xie, Yan-Xin Li, Xiang-Tao Shang et al. (2019) Effect of heat input on porosity defects in a fiber laser welded socket-Joint made of powder metallurgy molybdenum alloy. *Materials,* **12**, 1433. DOI: https://doi.org/10.3390/

ma12091433 https://www.semanticscholar.org/paper/Effect-of-Heat-Input-on-Porosity-Defects-in-a-Fiber-Xie-Li/ff3980832c812389e46ff4ffb4fe22d56e40a494
6. Zhang, L.J., Liu, J.Z., Pei, J.Y. et al. (2019) Effects of power modulation, multipass remelting and Zr addition upon porosity defects in laser seal welding of end plug to thin-walled molybdenum alloy. *J. Manuf. Process.,* **41**, 197–207. DOI: https://doi.org/10.1007/s00170-020-06482-5
7. Xie, M.X., Li, Y.X., Shang, X.T. et al. (2019) Microstructure and mechanical properties of a fiber welded socket-joint made of powder metallurgy molybdenum alloy. *Metals*, **9**, 640. DOI: https://doi.org/10.3390/met9060640
8. Zhang, L.L., Zhang, L.J., Long, J. et al. (2019) Enhanced mechanical performance of fusion zone in laser beam welding joint of molybdenum alloy due to solid carburizing. *Mater. Des*., **181**, 107957. DOI: https://doi.org/10.1016/j.matdes.2019.107957
9. Zhang, L.L., Zhang, L.J., Long, J. et al. (2019) Effects of titanium on grain boundary strength in molybdenum laser weld bead and formation and strengthening mechanisms of brazing layer. *Mater. Des.,* **169**, 107681. https://www.sciencedirect.com/science/article/pii/S0264127519301182 https://doi.org/10.1016/j.matdes.2019.107681
10. Mushegyan, V.O. (2009) Electron beam melting of reduced molybdenum concentrate. *Advances in Electrometallurgy,* **4**, 225–228.
11. Krajnikov, A.V., Morito, F., Slyunyaev, V.N. (1997) Impurity-induced embrittlement of heat-affected zone in welded Mo-based alloys. *Inter. J. of Refractory Metals and Hard Materials,* 15(**5–6**), 325–339. DOI: https://doi.org/10.1016/S0263-4368(97)87507-5
12. Stütz, M., Oliveira, D., Rüttinger, M. et al. (2016) Electron beam welding of TZM sheets. *Mater. Sci. Forum*, **879**, 1865–1869. DOI: https://doi.org/10.4028/www.scientific.net/MSF.879.1865
13. Korneev, N.I., Pevzner, S.B., Razuvaev, E.I., Skugarev, I.G. (1967) *Pressure processing of refractory metals and alloys*. Moscow, Metallurgiya [in Russian].
14. *Wang* Jiteng, Wang Juan, Li Yajiang and Zheng Deshuang (2014) Progress of research on welding for molybdenum alloys. *High Temp. Mater. Proc.* 33(**3**), 193–200. DOI: https://doi.org/10.1515/htmp-2013-0037
15. https://www.researchgate.net/publication/272570992_Progress_of_Research_on_Welding_for_Molybdenum_Alloys14
16. Skryabinskyi, V.V., Nesterenkov, V.M., Rusynyk, M.O. (2020) Electron beam welding with programming of beam power density distribution. *The Paton Welding J.,* **1**, 49–53. DOI: https://doi.org/10.37434/tpwj2020.01.07
17. Kovbasenko, S.N., Yakubovsky, V.V., Ivashchenko, G.A. et al. (1987) *Method of electron beam welding of high-strength steels*. USSR Cert. 1355411, Int. Cl. 3 V23K 15/00. PWI [in Russian].

ORCID
V.I. Zagornikov: 0000-0003-0456-173X,
V.M. Nesterenkov: 0000-0002-7973-1986,
K.S. Khripko: 0000-0002-4893-5441

CONFLICT OF INTEREST
The Authors declare no conflict of interest

CORRESPONDING AUTHOR
V.I. Zagornikov
E.O. Paton Electric Welding Institute of the NASU
11 Kazymyr Malevych Str., 03150, Kyiv, Ukraine.
E-mail: zagornikov@technobeam.com.ua

SUGGESTED CITATION
V.I. Zagornikov, V.M. Nesterenkov, K.S. Khripko, O.N. Ignatusha (2025) Electron beam welding of gas valve elements from Mo–Ti–Zr alloy. *The Paton Welding J*., **4**, 27–36.
DOI: https://doi.org/10.37434/tpwj2025.04.05

JOURNAL HOME PAGE
https://patonpublishinghouse.com/eng/journals/tpwj

Received: 20.06.2024
Received in revised form: 25.10.2024
Accepted: 09.05.2025